



# Biosynthesis of resolvin D1, resolvin D2, and RCTR1 from 7,8(S,S)-epoxytetraene in human neutrophils and macrophages

Robert Nshimiyimana<sup>a</sup> , Mélissa Simard<sup>a</sup> , Tarvi Teder<sup>b</sup> , Ana R. Rodriguez<sup>c</sup> , Bernd W. Spur<sup>c</sup> , Jesper Z. Haeggström<sup>b</sup> , and Charles N. Serhan<sup>a,1</sup>

Affiliations are included on p. 10.

Edited by Lawrence Steinman, Stanford University, Stanford, CA; received March 22, 2024; accepted July 29, 2024

While the acute inflammatory response to harmful stimuli is protective, unrestrained neutrophil swarming drives collateral tissue damage and inflammation. Biosynthesized from omega-3 essential polyunsaturated fatty acids, resolvins are a family of signaling molecules produced by immune cells within the resolution phase to orchestrate return to homeostasis. Understanding the mechanisms that govern biosynthesis of these potent molecules gives insight into stimulating endogenous resolution and offers fresh opportunities for preventing and treating excessive inflammation. In this report, using materials prepared by total synthesis and liquid chromatography and tandem mass spectrometry-based matching studies, we established the role of 7,8(S,S)-epoxytetraene intermediate in the biosynthesis of resolvin D1, resolvin D2, and the resolvin conjugate in tissue regeneration (RCTR1) by human phagocytes. We demonstrated that this 7,8(S,S)-epoxy-containing intermediate is directly converted to resolvin D2 by human M2-like macrophages and to resolvin D1 and RCTR1 by human macrophages, neutrophils, and peripheral blood mononuclear cells. In addition, both human recombinant soluble epoxide hydrolase (sEH) and the glutathione S-transferase leukotriene C<sub>4</sub> synthase (LTC<sub>4</sub>S) each catalyze conversion of this epoxide to resolvin D1 and RCTR1, respectively. MS<sup>3</sup> ion-trap scans and isotope incorporation of <sup>18</sup>O from H<sub>2</sub><sup>18</sup>O with sEH indicated that the oxygen atom at C-8 in resolvin D1 is derived from water. Results from molecular docking simulations with biosynthetic precursor 17S-hydroperoxy-4,7,10,13,19-*cis-15-trans*-docosahexaenoic acid and the epoxy intermediate were consistent with 5-lipoxygenase production of resolvin D1. Together, these results give direct evidence for the role of resolvin 7,8(S,S)-epoxytetraene intermediate in the endogenous formation of resolution-phase mediators resolvin D1, resolvin D2, and RCTR1 by human phagocytes.

inflammation resolution | innate immunity | macrophages | lipid mediators

Uncontrolled inflammation is now widely recognized as a critical component in the pathogenesis of many human afflictions, including neurodegenerative diseases, cardiovascular diseases, and metabolic syndrome (1). In 2002, a novel family of potent bioactive mediators from docosahexaenoic acid (DHA, C22:6, ω-3) were uncovered in resolving inflammatory exudates (2). These endogenous mediators were coined resolvins that function as stop signals and regulators of multicellular events without evoking immunosuppression (3). Failure to produce these local signaling molecules in animal disease models is associated with excessive inflammation, organ damage, and disease progression (3). The discovery of resolvins and related specialized pro-resolving lipid mediators (SPMs) (3) marked a new paradigm for termination of the acute inflammatory response and provided evidence that resolution is not a passive biochemical process as once widely believed (4).

Total organic synthesis plays a critical role in the structural elucidation and synthesis of chemical mediators and their analogs. Notably, conclusive evidence on the structure and biosynthesis of leukotrienes (LTs) was intimately linked to the chemical synthesis of LTA<sub>4</sub> (5). This transient allylic epoxide intermediate is common to both cysteinyl-leukotrienes, potent bronchoconstrictors, and leukotriene B<sub>4</sub>, a potent leukocyte chemoattractant. These studies contributed to the foundation of our understanding of the arachidonate pathway and led to therapeutic discoveries including the development of medicines such as montelukast and zileuton (6, 7). The biosynthesis of resolvins from essential polyunsaturated fatty acid DHA was initially postulated to arise from short-lived epoxy-containing intermediates (2). To this end, recent results confirmed the endogenous production of resolvin D3 (4S,11R,17S-trihydroxy-5Z,7E,9E,13Z,15E,19Z-docosahexaenoic acid) and resolvin D4 (4S,5R,17S-trihydroxy-6E,8E,10Z,13Z,15E,19Z-docosahexaenoic acid) to ensue via a conjugated triene 4,5(S,S)-epoxyresolvin (4S,5S-oxido-17S-hydroxy-6E,8E,10Z,13Z,15E,19Z-docosahexaenoic acid) intermediate (8, 9).

## Significance

It is now widely appreciated that inflammation contributes to many human conditions that were not thought to involve inflammation, e.g., aging, cardiovascular disease, metabolic syndrome, and neurodegenerative diseases. Uncovering previously unknown processes in human cells that control excessive inflammation is of both general and public health interest. Resolvins are molecules of the body's own resolution response that stops inflammation and protects organs. It is of broad interest to elucidate biochemical processes that lead to production of these highly potent molecules. Here, using synthetic resolvin 7,8(S,S)-epoxytetraene, we elucidate the central role of this intermediate in human blood cells as a precursor to resolvin D1, D2, and resolvin conjugate in tissue regeneration (RCTR1). These findings provide coordinates necessary for up-to-date pro-resolving therapies.

Author contributions: R.N. and C.N.S. designed research; R.N., M.S., T.T., and A.R.R. performed research; A.R.R., B.W.S., and J.Z.H. contributed new reagents/analytic tools; R.N., M.S., and C.N.S. analyzed data; and R.N. and C.N.S. wrote the paper.

Competing interest statement: C.N.S. is inventor on patents for resolvin D1, D2, and RCTRs that are assigned and managed by BWH. The other authors declare no competing interest.

This article is a PNAS Direct Submission.

Copyright © 2024 the Author(s). Published by PNAS. This article is distributed under [Creative Commons Attribution-NonCommercial-NoDerivatives License 4.0 \(CC BY-NC-ND\)](https://creativecommons.org/licenses/by-nc-nd/4.0/).

<sup>1</sup>To whom correspondence may be addressed. Email: cserhan@bwh.harvard.edu.

This article contains supporting information online at <https://www.pnas.org/lookup/suppl/doi:10.1073/pnas.2405821121/-/DCSupplemental>.

Published September 5, 2024.

Methoxy trapping products with activated human neutrophils implicated that the biosynthesis of resolvin D1 (7S,8R,17S-trihydroxy-4Z,9E,11E,13Z,15E,19Z-docosahexaenoic acid) occurs via a conjugated tetraene 7,8-oxirane (10). Based on this evidence, it was surmised that formation of resolvin D2 (7S,16R,17S-trihydroxy-4Z,8E,10Z,12E,14E,19Z-docosahexaenoic acid) and the C8-linked cysteinyl-resolvin (8R-glutathionyl-7S,17S-dihydroxy-4Z,9E,11E,13Z,15E,19Z-docosahexaenoic acid) could also proceed via this shared epoxide biosynthetic intermediate.

SPMs display beneficial roles in many widely occurring diseases, ranging from acute respiratory distress syndrome and COVID-19 infections to atherosclerosis (1), cardiovascular diseases, metabolic syndrome, and pain (3, 11). Recently, Lopez-Vicario et al. showed that DHA-derived autacoids, namely resolvin D1, rescue hepatocytes from TNF $\alpha$ -stimulated mitochondrial dysfunction, thus reprogramming optimal hepatic and metabolic energy efficiency (12). Circulating resolvin D1 and DHA are markedly decreased in patients with acutely symptomatic carotid disease (13), aneurysmal subarachnoid hemorrhage (14) and intracerebral brain hemorrhage (15), implying these molecules may be clinically significant. The resolvin D2-GPR18 signaling axis is protective in metabolic and cardiovascular diseases (16), and a recent human population study of 2,633 subjects demonstrated that both lower and higher levels of plasma resolvin D2 are associated with a reduced risk of atherosclerotic cardiovascular disease (17). RCTR1 limits human polymorphonuclear cell migration and stimulates bacterial and apoptotic neutrophil phagocytosis by monocyte-derived macrophages (18). Each of the resolvins has proven robust potent functions, e.g., resolvin D1 and D2 display antidepressant actions (19), resolvin D1 resolves atrial fibrillation in the heart (20), and RCTR1 is protective in acute respiratory distress syndrome (ARDS) (21). These beneficial functions in resolving inflammation and infections, in addition to other biological actions (3), emphasize the importance of elucidating the complete biosynthetic pathways that govern resolvin formation.

Herein, we report the role of resolvin 7,8(S,S)-epoxytetraene and demonstrate its biotransformation to resolvin D1, resolvin D2, and RCTR1 by isolated human leukocytes and recombinant enzymes. We also disclose that 17S-hydroperoxy-4,7,10,13,19-*cis*-15-*trans*-docosahexaenoic acid, 17S-H(p)DHA, a precursor to the 7,8(S,S)-epoxytetraene intermediate, is converted to both resolvin D1 and resolvin D2 by human phagocytes. Molecular docking simulations between 5-LOX and 17-H(p)DHA or 17-HDHA revealed that each of these ligands occupies the active binding pocket in a head-to-tail orientation, allowing hydrogen abstraction at C-9 and suggesting subsequent formation of the epoxy group at carbons C-7 and C-8. These computational studies also indicated that 7,8(S,S)-epoxytetraene binds into the human soluble epoxide hydrolase (sEH), giving favorable interactions between the epoxy ring and catalytic residues. Together, these results provide insights into the biosynthetic mechanisms in specific human leukocytes that produce the potent biologically active resolvins.

## Results

**Resolvin D1, D2, and RCTR1 Are Biosynthesized from 7,8(S,S)-Epoxytetraene.** To obtain direct evidence on the role of resolvin 7,8(S,S)-epoxytetraene in the formation of naturally occurring lipid mediators, we employed stereochemically pure materials obtained using two independent total syntheses. The first strategy was devised based on chirally catalyzed transformations and involved a triethylsilyl (TES) ether-protecting group, with the C<sub>1</sub>-C<sub>13</sub> epoxydienal and the C<sub>14</sub>-C<sub>22</sub> phosphonium bromide identified

as the key building blocks to furnish the target compound in a convergent manner (Fig. 1 *A, Left*). The purity of this material was greater than 99% as judged by straight-phase HPLC (Fig. 1 *A, Middle*), and this compound gave a UV (hexane/triethylamine, 10: 0.1, *v/v*) spectrum with a triplet band of absorption at  $\lambda_{\text{max}}$  294, 308, 322 nm, characteristic of a conjugated epoxy-tetraene chromophore (Fig. 1 *A, Right*). The second synthesis used a chiral pool-based approach with a *tert*-butyldiphenylsilyl (TBDPS)-protecting group (22). This compound was characterized by <sup>1</sup>H and <sup>13</sup>C NMR to confirm its complete structure and olefinic geometry (*SI Appendix, Fig. S1A*). In addition, RCTR1, RCTR2, and RCTR3 (18) were each obtained by opening the epoxytetraene with reduced glutathione, L-cysteinylglycine, and L-cysteine, respectively, giving further evidence of its intact oxirane and correct double bond configuration (*SI Appendix, Fig. S1B*). Prior to conducting studies with isolated cells and recombinant enzymes, the protected epoxytetraene was subjected to silyl group removal and ester hydrolysis (*Methods*).

With synthetic resolvin 7,8(S,S)-epoxytetraene at hand, we first investigated its conversion with isolated human leukocytes (Fig. 1). When suspensions of human polymorphonuclear neutrophils (PMNs) were incubated with the epoxy intermediate, two major products were formed as revealed by liquid chromatography and tandem mass spectrometry (LC-MS/MS)-based studies (Fig. 1*B*, red trace). The first product eluted at retention time (*T<sub>R</sub>*) 10.31 min while the second peak (*I*) was a minute apart at 11.33 min (Fig. 1*B*, red trace). Analytical data obtained from the first chromatographic signal at *T<sub>R</sub>* = 10.31 min were essentially identical to those of the synthetic resolvin D1, as confirmed by co-elution and MS/MS fragmentation. The tandem mass spectrum of this product showed key fragment ions characteristic of resolvin D1 including a parent molecular ion at *m/z* 375 = M-H and daughter ions at *m/z* 357 = M-H-H<sub>2</sub>O, *m/z* 233, *m/z* 215 = 233-H<sub>2</sub>O, *m/z* 197 = 233-2H<sub>2</sub>O, *m/z* 171, *m/z* 141, and *m/z* 135 = 171-2H<sub>2</sub>O (Fig. 1 *C, Left*). The second chromatographic product (*I*) at *T<sub>R</sub>* = 11.33 min possessed only an indistinguishable MS/MS fragmentation spectrum to resolvin D1, confirming it as a trihydroxy acid and presumably a closely related stereoisomer(s) that arose from nonenzymic aqueous hydrolysis of the 7,8-epoxide (Fig. 1*B*, purple trace, and *SI Appendix, Fig. S1C*).

Given the critical role that monocyte-derived macrophages play in the innate immune response and resolution of inflammation (8), we next investigated whether mononuclear leukocytes transform resolvin 7,8(S,S)-epoxytetraene to bioactive lipid mediators. Analyses of incubation materials of the epoxy intermediate with human M2-like macrophages revealed the formation of both resolvin D1 (*T<sub>R</sub>* = 10.35 min) and resolvin D2 (*T<sub>R</sub>* = 9.96 min) (Fig. 1*B*, blue trace). These incubations also led to the formation of product *I* (*T<sub>R</sub>* = 11.36 min). Both resolvin D1 and resolvin D2 matched the chromatographic retention times and MS/MS fragment ions to their respective synthetic versions. M2-like macrophage-derived resolvin D1 gave prominent ions including a parent ion at *m/z* 375 = M-H and daughter ions at *m/z* 357 = M-H-H<sub>2</sub>O, *m/z* 313 = M-H-H<sub>2</sub>O-CO<sub>2</sub>, *m/z* 233, *m/z* 215 = 233-H<sub>2</sub>O, *m/z* 197 = 233-2H<sub>2</sub>O, *m/z* 141, and *m/z* 135 = 171-2H<sub>2</sub>O (*SI Appendix, Fig. S1D*), and resolvin D2 displayed a molecular ion at *m/z* 375 = M-H and fragment ions at *m/z* 357 = M-H-H<sub>2</sub>O, *m/z* 339 = M-H-2H<sub>2</sub>O, *m/z* 313 = M-H-H<sub>2</sub>O-CO<sub>2</sub>, *m/z* 295 = M-H-2H<sub>2</sub>O-CO<sub>2</sub>, *m/z* 259 = 277-H<sub>2</sub>O, *m/z* 233, *m/z* 215 = 233-H<sub>2</sub>O, *m/z* 203 = 247-CO<sub>2</sub>, *m/z* 197 = 233-2H<sub>2</sub>O, *m/z* 175, and *m/z* 141 (Fig. 1 *C, Right*).

When the synthetic epoxytetraene intermediate was incubated with human peripheral blood mononuclear cells (PBMCs), we observed predominant formation of resolvin D1 (Fig. 1*B*, green

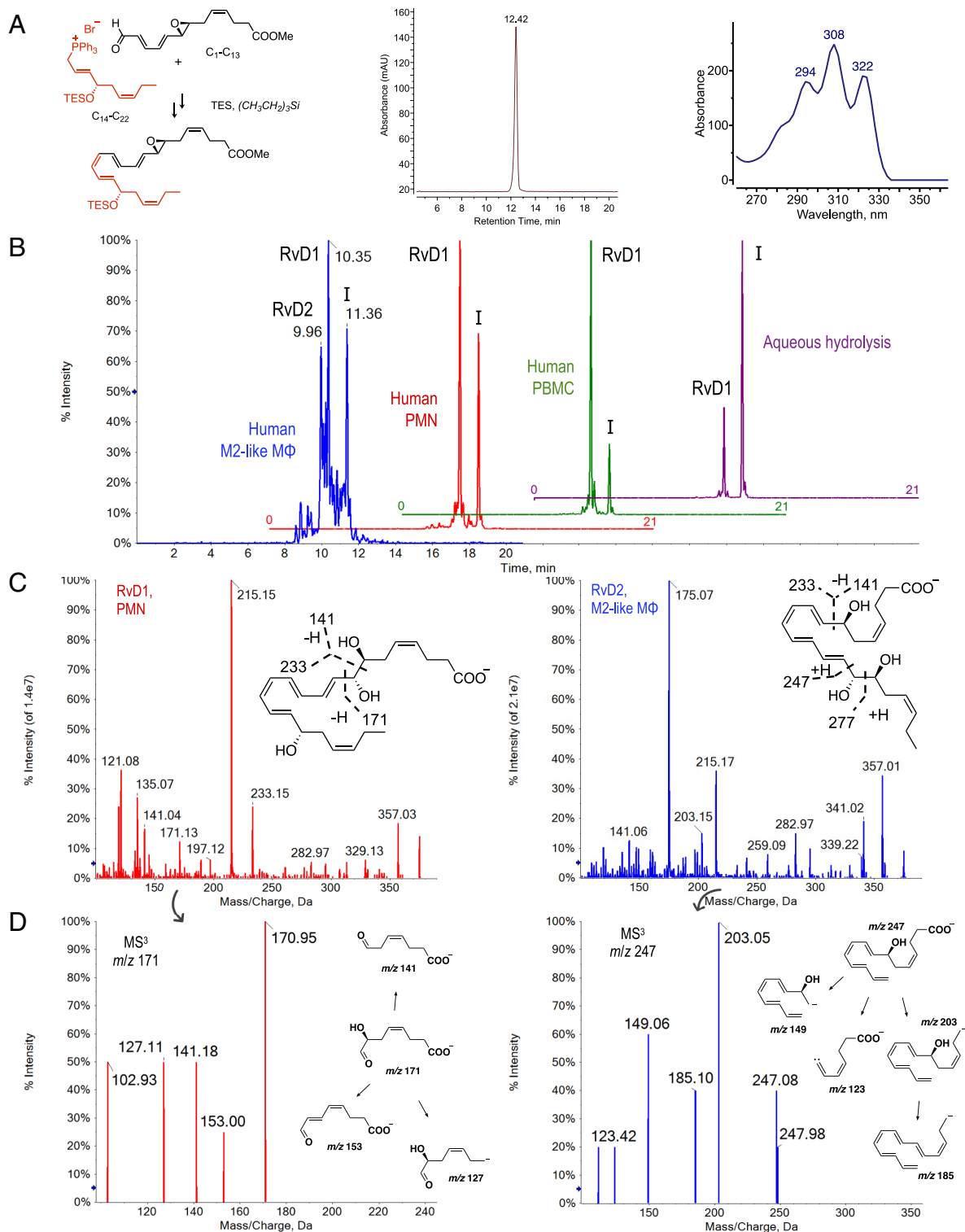


**Fig. 1.** Human phagocytes convert resolvin 7,8(S,S)-epoxytetraene to resolvin D1 and resolvin D2. (A) *Left*, Convergent retrosynthetic analysis of resolvin 7,8(S,S)-epoxytetraene in its protected form from epoxydienal C<sub>1</sub>-C<sub>13</sub> and phosphonium bromide C<sub>14</sub>-C<sub>22</sub> key building blocks. *Middle*, HPLC chromatogram of the purified epoxide under straight-phase conditions using hexane/Et<sub>3</sub>N (99/1, v/v) on a Phenomenex Luna-Si 250 × 10 mm column. *Right*, corresponding UV spectrum (hexane/Et<sub>3</sub>N, 99/1) showing a triplet band of absorption at λ<sub>max</sub> 294, 308, 322 nm. (B) Overlaid MRM chromatograms showing conversion of 7,8(S,S)-epoxytetraene to resolvin D1 (T<sub>R</sub> = 10.35 min) and resolvin D2 (T<sub>R</sub> = 9.96 min) by human M2-like macrophages (blue trace), to resolvin D1 (T<sub>R</sub> = 10.31 min) by freshly isolated human PMN (red trace), and to resolvin D1 (T<sub>R</sub> = 10.31 min) by human PBMC (green trace). All cell types generated trihydroxy acid I (T<sub>R</sub> = 11.36 min), a major product resulting from nonenzymatic aqueous hydrolysis of 7,8(S,S)-epoxytetraene in DPBS<sup>+/+</sup> buffer (pH = 7.45, 37 °C, 30 min). (C) *Left to Right*, Representative MS/MS spectra of leukocyte-derived resolvin D1 (parent ion at m/z 375 = M-H and daughter ions at m/z 357 = M-H-H<sub>2</sub>O, m/z 313 = M-H-H<sub>2</sub>O-CO<sub>2</sub>, m/z 295 = M-H-2H<sub>2</sub>O-CO<sub>2</sub>, m/z 233, m/z 215 = 233-H<sub>2</sub>O, m/z 197 = 233-2H<sub>2</sub>O, m/z 171, m/z 141, and m/z 135 = 171-2H<sub>2</sub>O) and resolvin D2 (m/z 375 = M-H, m/z 357 = M-H-H<sub>2</sub>O, m/z 313 = M-H-H<sub>2</sub>O-CO<sub>2</sub>, m/z 295 = M-H-2H<sub>2</sub>O-CO<sub>2</sub>, m/z 259 = 277-H<sub>2</sub>O, m/z 233, m/z 215 = 233-H<sub>2</sub>O, m/z 197 = 233-2H<sub>2</sub>O, m/z 175, and m/z 141). (D) *Left to Right*, MS<sup>3</sup> spectra of resolvin D1 and resolvin D2 diagnostic ions at m/z 171 and m/z 247 and their proposed downstream second-generation product ions. Retention times and MS/MS spectra of leukocyte-derived resolvin D1 and D2 were essentially identical to those of synthetic reference materials. Overlaid MRM chromatograms are presented as screen captures taken from SCIEX OS-Q (explorer mode) with offset traces in X and Y-axes using 20.0% and 5.0% of range, respectively. Results from incubations represent n = 3 different healthy volunteers. HPLC, high-performance liquid chromatography; MRM, multiple reaction monitoring; PMNs, polymorphonuclear neutrophils; PBMCs, peripheral blood mononuclear cells.



trace) and this product cochromatographed with synthetic resolvin D1. Its corresponding MS/MS spectrum also gave essentially identical fragmentation pattern to resolvin D1 with a molecular ion at  $m/z$  375 = M-H and daughter ions at  $m/z$  357 = M-H-H<sub>2</sub>O,  $m/z$  241 = 277-H<sub>2</sub>O,  $m/z$  233,  $m/z$  215 = 233-H<sub>2</sub>O,  $m/z$  171,  $m/z$  141, and  $m/z$  135 = 171-2H<sub>2</sub>O (*SI Appendix, Fig. S1E*). Taking advantage of the linear accelerator trap functionality, we obtained MS/MS/MS (MS<sup>3</sup>) evidence by trapping, isolating, and further fragmenting specific ions of interest, viz.,  $m/z$  171 and  $m/z$  247. As seen in Fig. 1D, the linear ion trap (LIT) fragmentation of  $m/z$  171, a unique ion for resolvin D1, yielded a range of second-generation product ions including  $m/z$  153,  $m/z$  141, and  $m/z$  127 (Fig. 1D, *Left*). Similarly, MS<sup>3</sup> of  $m/z$  247, a signature ion of resolvin D2, generated key downstream product ions at  $m/z$  203,  $m/z$  185,  $m/z$  149, and  $m/z$  123 (Fig. 1D, *Right*). These results provided advanced confirmatory evidence of resolvin D1 and D2 production in human PMNs and M2-like macrophages, owing to the high selectivity and specificity of these in-trap fragmentation scans.

Cysteinyl-SPMs such as RCTR1 are multifunctional mediators with organ-protective and tissue-regenerative functions (18). We sought evidence whether this potent molecule is biosynthesized via the 7,8(S,S)-epoxytetraene intermediate by human phagocytes. To this end, extracts obtained from incubations of human M2-like macrophages, PMNs, and PBMCs were subjected to mass spectrometry-based data acquisition and analyses in positive ionization mode to monitor the formation of cysteinyl-containing products. LC-MS/MS analyses showed production of RCTR1 from the epoxy-intermediate by human phagocytes as evidenced by chromatographic MRMs and MS/MS fragmentation spectra that matched synthetic RCTR1. As seen in Fig. 2A, *Left*, blue trace, human neutrophil incubations revealed formation of a predominant product at  $T_R$  = 8.32 min, and this chromatographic signal gave a corresponding fragmentation spectrum with  $m/z$  666 = M+H,  $m/z$  648 = M+H-H<sub>2</sub>O,  $m/z$  630 = M+H-2H<sub>2</sub>O,  $m/z$  506 = 524-H<sub>2</sub>O,  $m/z$  501 = 537-2H<sub>2</sub>O,  $m/z$  398 = 434-2H<sub>2</sub>O,  $m/z$  323 = 359-2H<sub>2</sub>O, and  $m/z$  185 = 203-H<sub>2</sub>O, characteristic of RCTR1 (Fig. 2A, *Right*). In addition, both human PBMC and M2-like macrophages (Fig. 2A, *Left*, red trace and *SI Appendix, Fig. S2A*) also biosynthesized RCTR1 from this 7,8(S,S)-epoxy intermediate, as evidenced by matching chromatography and fragmentation spectra.

Along these lines, it is well documented that glutathione S-transferases (GSTs) stereoselectively add reduced glutathione (GSH) to fatty acid epoxides to biosynthesize cysteinyl-containing mediators such as 4S,5R-RCTR1 (8, 23) and cysteinyl-leukotrienes (24). Using a well-known GST, leukotriene C<sub>4</sub> synthase (LTC<sub>4</sub>S), we examined whether the human recombinant enzyme directly utilizes the 7,8(S,S)-epoxytetraene to form RCTR1. As shown in *SI Appendix, Fig. S2B*, the authentic RCTR1 cochromatographed with the enzymatically derived material. Further, tandem mass spectrometric data of synthetic and biogenic products gave consistent and identical prominent ions with parent ion of  $m/z$  666 = M+H and daughter ions at  $m/z$  630 = M+H-2H<sub>2</sub>O,  $m/z$  506 = 524-H<sub>2</sub>O,  $m/z$  501 = 537-2H<sub>2</sub>O,  $m/z$  398 = 434-2H<sub>2</sub>O,  $m/z$  323 = 359-2H<sub>2</sub>O, and  $m/z$  203 (*SI Appendix, Fig. S2B*). Together, these results establish the pivotal role of resolvin 7,8(S,S)-epoxytetraene as intermediate in the stereoselective biosynthesis of resolvin D1, resolvin D2, and RCTR1 by human phagocytes.

**Mechanism of Resolvin 7,8(S,S)-Epoxytetraene Biosynthesis.** The 17S-mono-oxygenation product of DHA, 17S-H(p)DHA, serves as a precursor to 17S-resolvins (25). Therefore, we questioned

whether, in the presence of 5-lipoxygenase (5-LOX) and an epoxide hydrolase, this substrate is transformed to resolvin D1 via the 7,8(S,S)-epoxytetraene intermediate. To this end, using a cell-free system with isolated enzymes, incubation of 17S-H(p)DHA with potato 5-LOX and human recombinant sEH led to the formation of resolvin D1 ( $T_R$  = 10.30 min) and the nonenzymatic hydrolysis product I ( $T_R$  = 11.31 min) as indicated by LC-MS/MS (Fig. 2B, *Left*). Resolvin D1 was further confirmed by its fragmentation spectrum, which displayed a parent ion at  $m/z$  375 = M-H and fragment daughter ions at  $m/z$  357 = M-H-H<sub>2</sub>O,  $m/z$  339 = M-H-2H<sub>2</sub>O,  $m/z$  313 = M-H-H<sub>2</sub>O-CO<sub>2</sub>,  $m/z$  243 = 305-H<sub>2</sub>O-CO<sub>2</sub>,  $m/z$  233,  $m/z$  215 = 233-H<sub>2</sub>O,  $m/z$  197 = 233-2H<sub>2</sub>O,  $m/z$  171,  $m/z$  141, and  $m/z$  135 = 171-2H<sub>2</sub>O (*SI Appendix, Fig. S2C*). These results indicate formation of the 7,8(S,S)-epoxytetraene intermediate from 17S-H(p)DHA via concerted sequential activities of 5-LOX.

With these results, molecular modeling studies of 17S-H(p)DHA into the catalytic site of stable 5-LOX structure were undertaken (Fig. 2B, *Right*). This intermediate was docked into the active site of 5-LOX with the distance between the hydrogen abstraction site at C-9 and catalytic iron ranging between 5 and 6 Å. The distance of 17S-H(p)DHA from iron corresponds to the complex between arachidonic acid (AA) and 5-LOX (PDB ID: 3V99). In addition, the carboxy group of 17S-H(p)DHA gave polar interaction with Q413, and the hydroperoxy group was located close to Q363 and H360 residues, and stabilized by Q180 (Fig. 2B, *Right*). Fig. 2C is the proposed 5-LOX reaction mechanism converting 17S-H(p)DHA to 7,8(S,S)-epoxytetraene intermediate by successive elimination of the *D*-hydrogens at C-9 and C-12. Next, we incubated 17S-H(p)DHA with isolated human leukocytes. As seen in *SI Appendix, Fig. S2D*, incubations with freshly isolated PMNs gave rise to substantial formation of resolvin D2 ( $T_R$  = 9.96 min) and relatively low levels of resolvin D1 ( $T_R$  = 10.34 min) as well as additional trihydroxy acids including product I. Resolvin D2 was confirmed by matching of its retention time and MS/MS spectrum to the synthetic material. The biologically derived product gave a parent molecular ion at  $m/z$  375 = M-H and daughter ions at  $m/z$  357 = M-H-H<sub>2</sub>O,  $m/z$  331 = M-H-CO<sub>2</sub>,  $m/z$  313 = M-H-H<sub>2</sub>O-CO<sub>2</sub>,  $m/z$  295 = M-H-2H<sub>2</sub>O-CO<sub>2</sub>,  $m/z$  277,  $m/z$  259 = 277-H<sub>2</sub>O,  $m/z$  233,  $m/z$  215 = 233-H<sub>2</sub>O,  $m/z$  203 = 247-CO<sub>2</sub>,  $m/z$  197 = 233-2H<sub>2</sub>O,  $m/z$  175, and  $m/z$  141, consistent with synthetic resolvin D2 (*SI Appendix, Fig. S2D*). Given the prominent base peak observed in resolvin D2 MS<sup>2</sup> spectra at  $m/z$  175, we investigated and proposed possible structures for this collision-induced dissociation (CID) fragmentation ion using deuterium-labeled standards as detailed in *SI Appendix, Fig. S2E*.

In addition to 17S-H(p)DHA and 5-LOX docking studies (Fig. 2B), we explored the interactions of 5-LOX with DHA, 17S-hydroxy-DHA (17S-HDHA), 17R-H(p)DHA, and 17R-HDHA (*SI Appendix, Fig. S3 and Table S2*). Of interest, the docking of DHA into 5-LOX catalytic center resulted in two different orientations: head-to-tail in which the carboxy group of DHA interacted with Q413, or tail-to-head whereby the carboxy group of DHA interacted with R596 (*SI Appendix, Fig. S3A*). The head-to-tail pose presented the hydrogen abstraction site close to C-9 whereas the tail-to-head orientation was positioned closer to C-15. Conversely, simulations of 17-hydro(pero)xy products of DHA did not exhibit interactions with R596 and mostly bound to the catalytic center only in head-to-tail orientations (*SI Appendix, Fig. S3B–D*). These results illustrate that the 17-hydro(pero)xy group sterically hinders 17-H(p)DHA or 17-HDHA from binding in the tail-to-head position, allowing hydrogen abstraction at C-9, and favoring formation of the 7S-hydroperoxy-17S-HDHA

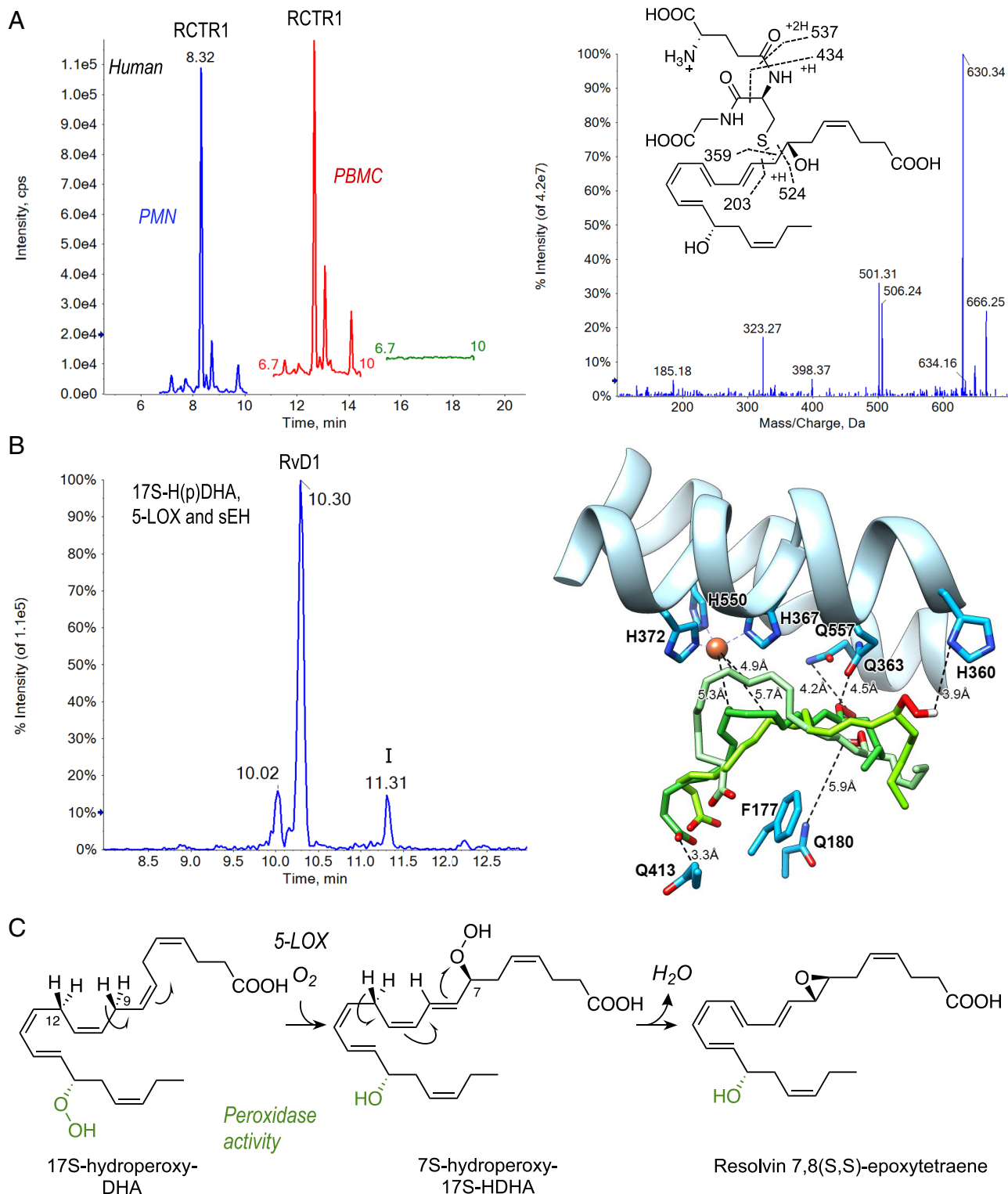


**Fig. 2.** Conversion of 7,8(S,S)-epoxytetraene to RCTR1 by human leukocytes and its formation from 17S-H(p)DHA by 5-lipoxygenase. (A) *Left*, Chromatographic MRMs acquired in positive ionization mode showing formation of RCTR1 ( $T_R = 8.32$  min) from incubations of 7,8(S,S)-epoxytetraene with human PMNs (blue trace) and PBMCs (red trace). The green trace shows a control experiment without added substrate to PBMCs. *Right*, Representative MS/MS spectrum of neutrophil-derived RCTR1 showing prominent and characteristic ions ( $m/z$  666 =  $M+H$ ,  $m/z$  648 =  $M+H-H_2O$ ,  $m/z$  630 =  $M+H-2H_2O$ ,  $m/z$  506 =  $524-H_2O$ ,  $m/z$  501 =  $537-2H_2O$ ,  $m/z$  398 =  $434-2H_2O$ ,  $m/z$  323 =  $359-2H_2O$ , and  $m/z$  185 =  $203-H_2O$ ). Both retention time and MS/MS fragmentation spectrum of the leukocyte-derived product matched those of synthetic RCTR1. (B) *Left*, MRM trace showing production of resolvin D1 ( $T_R = 10.30$  min) from potato 5-LOX (25 U) and human recombinant sEH (1  $\mu$ g) incubations with 17S-H(p)DHA (10  $\mu$ M) in phosphate buffer (pH = 7.4, 37  $^{\circ}$ C, 30 min). *Right*, Molecular docking simulations of 17S-H(p)DHA with 5-LOX X-ray crystal structure. The docking position for 17S-H(p)DHA was located close to the catalytic iron favoring hydrogen abstraction at C-9. The carboxy group of 17S-H(p)DHA gave polar interaction with Q413. The 17S-hydroperoxy group was located close to Q363 or H360 and was stabilized by Q180. Binding modes of 17S-H(p)DHA, catalytic iron, and interacting residues are presented in green, orange, and sky blue, respectively. (C) Proposed 5-LOX reaction mechanism for the formation of resolvin 7,8(S,S)-epoxytetraene from 17S-H(p)DHA by successive elimination of hydrogens at C-9 and C-12. MS/MS and MRM data are presented as screen captures from SCIEX OS-Q with offset traces in X and Y-axes using 20.0% and 5.0% of range, respectively, for the MRM chromatograms. Results from incubations represent  $n = 3$  separate experiments. MRM, multiple reaction monitoring; PMNs, polymorphonuclear neutrophils; PBMCs, peripheral blood mononuclear cells; RCTR, resolvin conjugate in tissue regeneration; 17S-H(p)DHA, 17S-hydroperoxy-4,7,10,13,19-cis-15-trans-docosahexaenoic acid; 5-LOX, 5-lipoxygenase.

intermediate (Fig. 2 *B* and *C*) and ultimately producing resolvin D5 (7S,17S-dihydroxy-4Z,8E,10Z,13Z,15E,19Z-docosahexaenoic acid) or resolvin D1 via 7,8(S,S)-epoxytetraene. Along these lines, it is well appreciated that fatty acid hydroperoxides increase lipooxygenase activity (26), and thus, at 5  $\mu$ M, the 17-H(p)DHA proved to be the more active substrate than 17-HDHA with isolated 5-LOX, as demonstrated by the formation of resolvin D5 (*SI Appendix, Fig. S3E*).

**Resolvin D1 Is Produced by Human Recombinant sEH.** It is well known that epoxide hydrolases such as the sEH convert leukotriene  $A_4$  to 5S,6R-DiHETE (27) and other fatty acid epoxides to their corresponding 1,2-diols by the addition of a molecule of water. Hence, we questioned whether the sEH is responsible for the biosynthesis of other lipid mediators that carry a vicinal diol group such as resolvin D1. To test this, we incubated the synthetic 7,8(S,S)-epoxytetraene in the presence of the sEH (human, recombinant). Analysis by LC-MS/MS revealed formation of two hydrolysis products that eluted at  $T_R = 10.36$  min and  $T_R = 11.36$  min (Fig. 3*A*). The predominant chromatographic peak at  $T_R = 10.36$  min matched its LC-MS/MS physical characteristics to synthetic resolvin D1 (Fig. 3*A* and *SI Appendix, Fig. S4*), whereas the signal at  $T_R = 11.36$  min proved to be the nonenzymatic aqueous hydrolysis product **I** (Fig. 1*B*, purple trace, and *SI Appendix, Fig. S1C*).

Tandem mass spectrometric spectra recorded in negative ionization for the sEH-derived resolvin D1 showed a molecular ion at  $m/z$  375 = M-H and fragment ions at  $m/z$  357 = M-H-H<sub>2</sub>O,  $m/z$  331 = M-H-CO<sub>2</sub>,  $m/z$  313 = M-H-H<sub>2</sub>O-CO<sub>2</sub>,  $m/z$  295 = M-H-2H<sub>2</sub>O-CO<sub>2</sub>,  $m/z$  259 = 277-H<sub>2</sub>O,  $m/z$  233,  $m/z$  215 = 233-H<sub>2</sub>O,  $m/z$  171,  $m/z$  141, and  $m/z$  135 = 171-2H<sub>2</sub>O (*SI Appendix, Fig. S4*). Furthermore, using a multistage fragmentation in the LIT, MS<sup>3</sup> scans of a diagnostic ion for resolvin D1, i.e.,  $m/z$  171, provided advanced evidence as indicated by the observed second-generation product ions and proposed fragments (*SI Appendix, Fig. S4*). Encouraged by these results, we performed molecular modeling experiments of resolvin 7,8(S,S)-epoxytetraene with the crystal structure of human sEH. The epoxytetraene occupied the binding pocket and showed favorable docking modes. Within distances of around 3 Å, the epoxy group interacted with critical catalytic residues Tyr381 and Tyr645, which carry out the hydrolysis of the epoxy group of fatty acid substrates (Fig. 3*A, Inset*). Additionally, the carboxylate faced toward Phe379, Gln383, Met337, and Asn471 residues, while the alcohol group gave potential hydrogen-hydrogen bond interactions with Asp495 and Met418.

**<sup>18</sup>O Incorporation from H<sub>2</sub><sup>18</sup>O.** The synthetic 7,8(S,S)-epoxytetraene is a *trans*-epoxide in an allylic position. It has been demonstrated that the mouse liver cytosolic epoxide hydrolase catalyzes the hydration of *trans*-epoxides in a stereospecific manner, yielding the corresponding *erythro*-diols (27). Additionally, given the increased electrophilicity of C-8 as a result of the proximal  $\Delta^9$  double bond, this position should in theory be more susceptible than C-7 to a nucleophilic attack by a molecule of water. The stereospecific hydrolysis would lead to the inversion of chirality at C-8 and retention at C-7, thus forming the 7S,8R-vicinal diol configuration present in resolvin D1.

With this postulate in mind, we tested whether enzymatic hydrolysis of the 7,8(S,S)-epoxytetraene with sEH in H<sub>2</sub><sup>18</sup>O-enriched buffer would preferentially incorporate the heavy isotope at the C-8 position. Upon analysis of the enzymatic product (resolvin D1-<sup>18</sup>O) by LC-MS/MS, changes in ion shift were observed that confirmed O<sup>18</sup>-insertion. As seen in Fig. 3*B*, the

parent molecular ion and fragments carrying the hydroxyl group from C-8 showed an increase of 2 mass units (Da), while those carrying the hydroxyl group from C-7 remained unchanged. The parent ion was found at  $m/z$  377 = M-H and daughter fragments at  $m/z$  359 = M-H-H<sub>2</sub>O, 341 = M-H-2H<sub>2</sub>O, 333 = M-H-CO<sub>2</sub>, 261 = 279-H<sub>2</sub>O, 245 = 307-H<sub>2</sub>O-CO<sub>2</sub>,  $m/z$  235, and 217 = 235-H<sub>2</sub>O,  $m/z$  173, and  $m/z$  141 (Fig. 3*B*). Additionally, O<sup>18</sup>-insertion was further examined using MS<sup>3</sup> studies of diagnostic fragment ions at  $m/z$  173, giving advanced evidence on the heavy oxygen insertion as depicted by the observed ions at  $m/z$  155 and  $m/z$  129 (Fig. 3*C*). These data suggest that <sup>18</sup>O incorporation is primarily directed at C-8 position and they support the stereospecific hydration of the 7,8(S,S)-epoxy intermediate to resolvin D1 by sEH.

## Discussion

In this report, we described the mechanism of formation of the potent bioactive lipid mediators resolvin D1, resolvin D2, and RCTR1 by human phagocytes via a common tetraenic 7,8(S,S)-epoxy-containing intermediate, as demonstrated using LC-MS/MS-based analyses (Figs. 1–3). This epoxide was prepared by total organic synthesis and was transformed to resolvin D2 by human M2-like macrophages, as well as resolvin D1 and RCTR1 by the M2-like macrophages, PMNs, and PBMCs (Figs. 1 and 2 and *SI Appendix, Fig. S2*). The products were identified via matching of their physical properties, i.e., chromatographic retention times and tandem mass spectral data, to those of synthetic materials (10, 18, 28). We also reported that human recombinant sEH and the GST leukotriene C4 synthase (LTC<sub>4</sub>S) each convert the epoxytetraene substrate to resolvin D1 and RCTR1, respectively (Fig. 3 and *SI Appendix, Fig. S2*).

Using multistage MS<sup>3</sup> and isotopic labeling studies of <sup>18</sup>O from H<sub>2</sub><sup>18</sup>O with sEH, we found that the oxygen atom at C-8 in resolvin D1 was derived from molecular water (Fig. 3), consistent with the sEH reaction mechanism (27). In addition, coinubations of 5-LOX and sEH with 17S-H(p)DHA produced resolvin D1 and the nonenzymatic aqueous hydrolysis product **I** (Fig. 2), providing additional evidence for the formation of the transient 7,8(S,S)-epoxytetraene as key biosynthetic intermediate. To examine this further using in silico studies, molecular docking simulations of 17S-H(p)DHA with the structure of 5-LOX gave polar interactions with key active site residues, namely Q413, Q363, H360 residues, and Q180, indicating hydrogen abstraction at C-9 and implicating formation of resolvin 7,8(S,S)-epoxytetraene (Fig. 2). Docking experiments of the epoxytetraene with the human sEH crystal structure also indicated favorable interactions with key catalytic residues Y381 and Y645 that carry out the hydrolysis of epoxy groups of fatty acid substrates.

DHA is the precursor to potent bioactive mediators that regulate key events in the resolution of inflammation (2, 25). The biosynthesis of resolvin D1, resolvin D2, and RCTR1 is initiated by oxygenation of DHA with 15-lipoxygenase (15-LOX) to produce 17S-H(p)DHA (25). Results presented here indicate that 17S-H(p)DHA undergoes a second lipoxygenation by 5-LOX to generate a C7-hydroperoxy-containing product, which is further transformed to a transient resolvin 7,8(S,S)-epoxytetraene intermediate (Figs. 2 and 4). Formation of the 7,8(S,S)-epoxytetraene involves sequential hydrogen abstraction by 5-LOX (Fig. 2), in an analogous manner to the formation of leukotriene  $A_4$  from arachidonic acid, as demonstrated by Shimizu et al. (*SI Appendix, Fig. S7*) (29). As illustrated in Fig. 4, in the presence of human leukocytes or recombinant enzyme, the 7,8(S,S)-epoxytetraene undergoes stereospecific hydrolysis with a molecule of water at



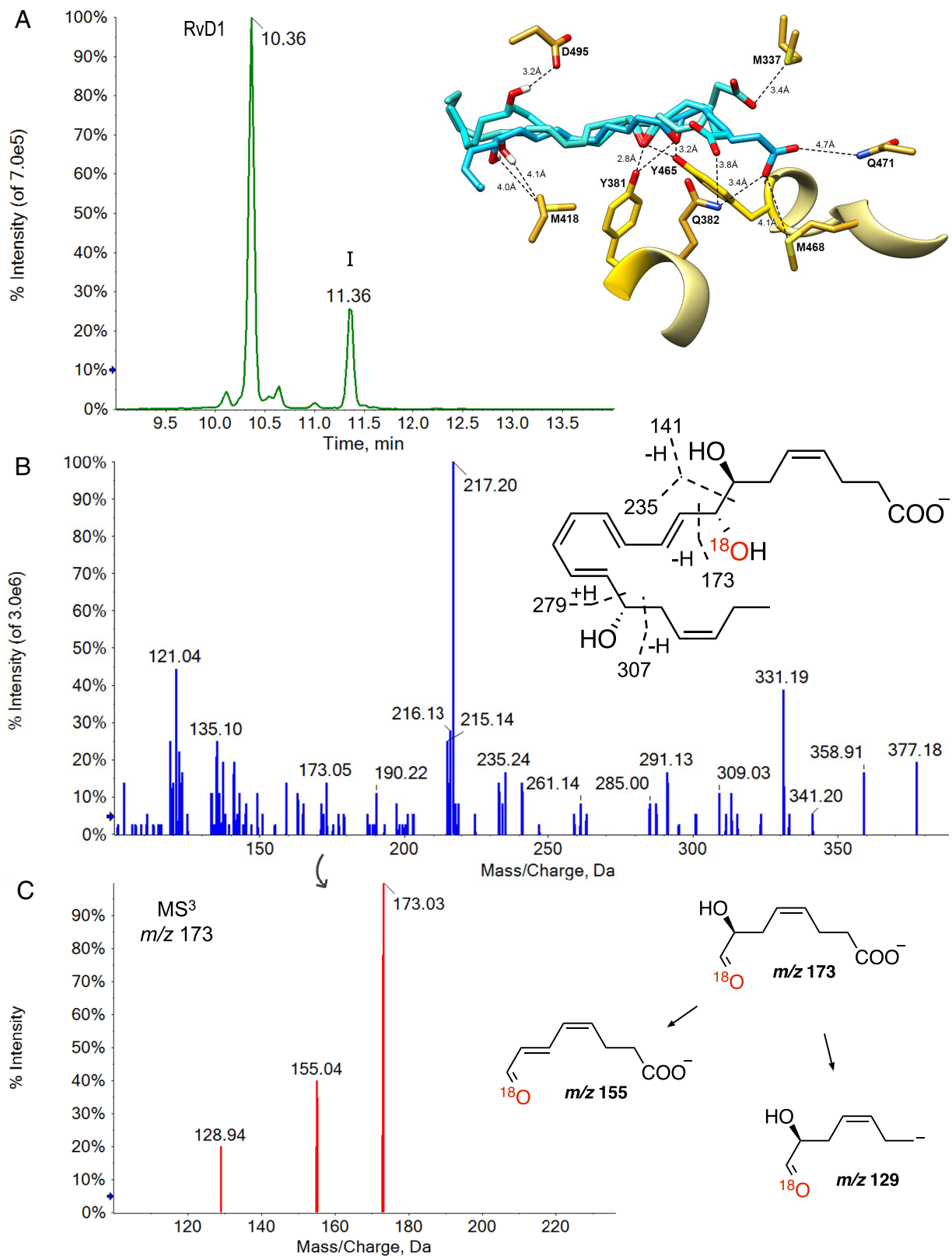


**Fig. 3.** Resolvin D1 is produced by human recombinant sEH. (A) *Left*, Chromatographic MRM trace showing formation of resolvin D1 ( $T_R = 10.36$  min) using rh sEH (0.2  $\mu$ M) and synthetic resolvin 7,8(S,S)-epoxytetraene (5  $\mu$ M) in tris-buffered saline (pH = 8, 37 °C, 30 min). These incubation conditions also generated the nonenzymatic aqueous hydrolysis product I ( $T_R = 11.36$  min) in relatively small amounts. These results are representative of  $n = 3$  separate experiments. *Right*, Computational modeling of resolvin 7,8(S,S)-epoxytetraene (blue) into the catalytic site of human crystal structure. The epoxy group gives interactions with key catalytic tyrosine residues Y381 and Y465 (yellow). (B) MS/MS spectrum of  $O^{18}$ -containing resolvin D1 produced from 7,8(S,S)-epoxytetraene intermediate by sEH in  $H_2O^{18}$ -enriched buffer. The molecular ion at  $m/z$  377 = M-H and daughter ions at  $m/z$  359 = M-H- $H_2O$ ,  $m/z$  333 = M-H- $CO_2$ ,  $m/z$  245 = 307- $H_2O$ - $CO_2$ ,  $m/z$  235, and  $m/z$  217 = 235- $H_2O$ ,  $m/z$  173, and  $m/z$  141 confirmed epoxy group opening and  $O^{18}$ -insertion, as judged by an increase of 2 daltons (Da) in fragment ions carrying the heavy isotope. (C) MS<sup>3</sup> spectrum of resolvin D1- $O^{18}$  diagnostic ion at  $m/z$  173 and its observed second-generation product ions at  $m/z$  155 and  $m/z$  129. Results from incubations are representative of  $n = 3$  separate experiments. sEH, soluble epoxide hydrolase (human, recombinant); MS<sup>3</sup>, MS/MS/MS.

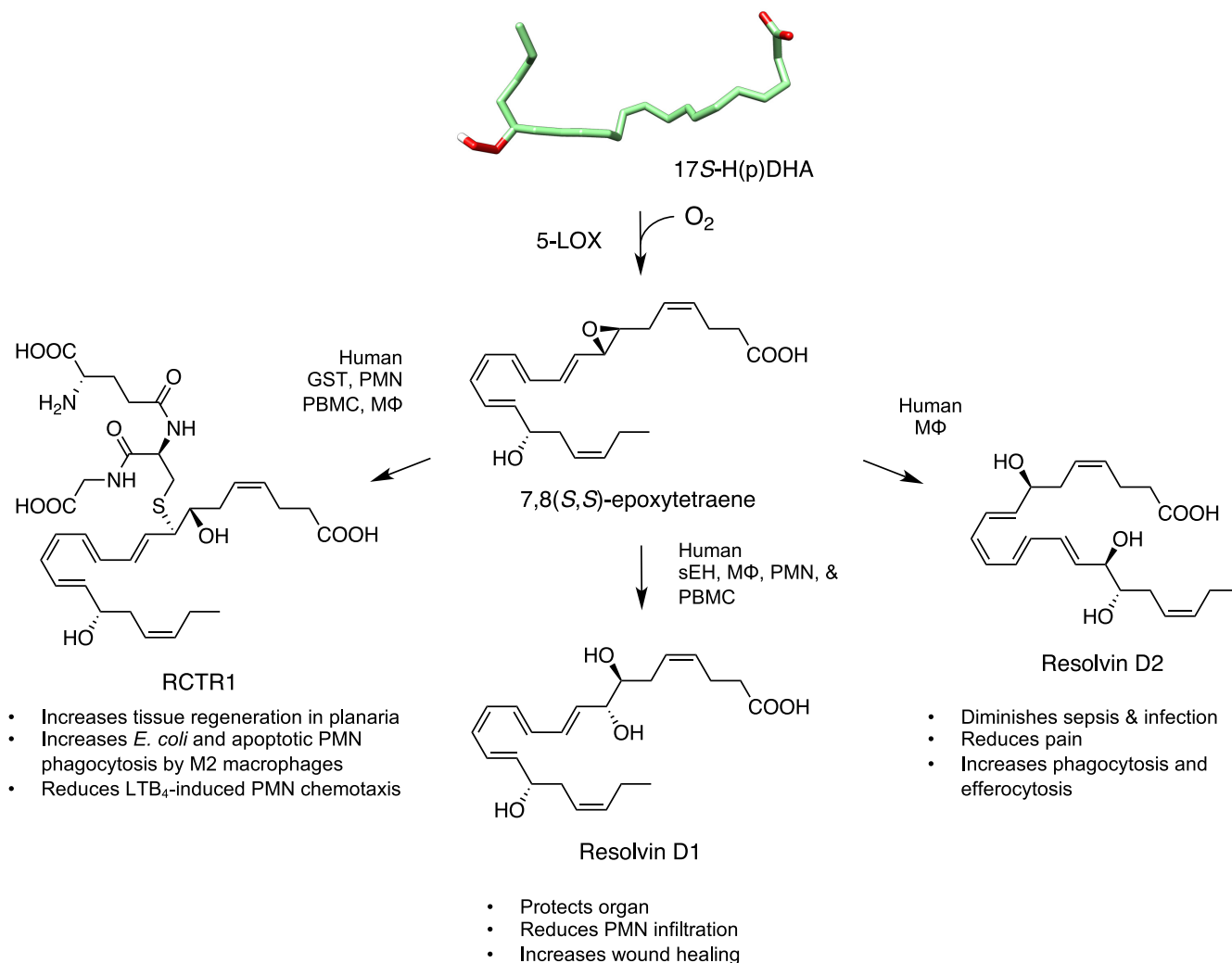


**Fig. 4.** Proposed biosynthesis of resolvins D1, D2, and RCTR1 via 7,8(S,S)-epoxytetraene intermediate. The 17S-hydroperoxy product of DHA undergoes oxygenation by 5-LOX to form resolvin 7,8(S,S)-epoxytetraene following a successive hydrogen abstraction reaction mechanism. This transient epoxy intermediate is further converted to potent bioactive mediators RCTR1 via GST, e.g., human recombinant LTC<sub>4</sub>S, and human leukocytes (neutrophils, PBMCs, and M2-like macrophages), resolvin D1 by human recombinant sEH and human PMN, PBMC, and M2, as well as resolvin D2 by human M2 cells. These autacoids are highly potent chemical mediators with a wide range of pro-resolving and organ-protective functions; see refs. 3 and 18 and text for details. Formation of resolvin D1 and resolvin D2 is proposed to ensue via an enzyme-bound delocalized cation formed by proton transfer, analogous to the carbonium intermediate proposed by E. J. Corey for lipoxin biosynthesis (30). RCTR1, resolvin conjugate in tissue regeneration 1; PMNs, polymorphonuclear neutrophils; PBMCs, peripheral blood mononuclear cells; sEH, soluble epoxide hydrolase (human, recombinant); LTC<sub>4</sub>S, leukotriene C<sub>4</sub> synthase (human, recombinant).

either carbon C-8 position to produce resolvin D1 by an  $S_N2$  mechanism or at position C-16 to generate resolvin D2 via a proposed enzyme-bound delocalized cation, in an analogous fashion to lipoxin biosynthesis (30). An enzymatic nucleophilic  $S_N2$  reaction with reduced glutathione opens this oxirane at the C-8 position, resulting in endogenous formation of RCTR1 (Fig. 4). Our present results indicate that a yet-to-be-identified hydrolase that can regiospecifically rearrange the double bond geometry is required to produce resolvin D2 from the 7,8(S,S)-epoxy intermediate by human M2-like macrophages (Figs. 1 and 4). PBMC preparations in the present experiments were ~69% monocytes and ~31% lymphocytes (*SI Appendix, Fig. S6*), and it is documented that PBMCs, macrophages, lymphocytes, and neutrophils each carry sEH (31) and thus can participate in resolvin D1 production when the 7,8(S,S)-epoxytetraene is present. Of particular interest, while the small-molecule inhibitors of sEH and LTC<sub>4</sub>S, TPPU, and TKO5, respectively, blocked production of resolvin D1 (*SI Appendix, Fig. S8*) and RCTR1 (*SI Appendix, Fig. S9*) in isolated neutrophils, PBMCs, as well as M1-like and M2-like macrophages, in vivo inhibition of sEH was

demonstrated to increase endogenous pro-resolving mediators in inflammation (32).

Stereochemical elucidation and biological evaluation of resolvin D1 demonstrated its potent actions in stopping transendothelial migration of human neutrophils ( $EC_{50} = 30$  nM) and in limiting leukocyte infiltration in murine peritonitis (10). Resolvin D1 activates the lipoxin A<sub>4</sub> receptor (ALX/FPR2), expressed on monocytes, macrophages, and neutrophils, leading to host defense mechanisms (33) including stimulation of macrophages toward a reparative phenotype, reduction of neutrophil chemotaxis, and regulation of cytokines by human M2-like macrophages, e.g., IL-13, IL-21, IL-8, IL-10 (*SI Appendix, Fig. S10*). Resolvin D1 also stimulates endogenous resolution processes (10) and is atheroprotective (34). Identification of stereochemistry and innate functions of resolvin D2 revealed its potent activities in reducing excessive neutrophil trafficking to the inflammatory milieu and in controlling microbial sepsis (28). Activation of the resolvin D2-GPR18 signaling axis induces M1 to M2 macrophage phenotype, stimulates nitric oxide production, reduces pro-inflammatory cytokines, e.g., IL-21, IL-13 (*SI Appendix, Fig. S10*), and plays a critical role in the resolution



of inflammation in cardiovascular diseases (16, 35). Along these lines, when added to M1-like macrophages, the 7,8(S,S)-epoxytetraene mildly stimulated polarization toward the M2-like phenotype by ~10% (*SI Appendix, Fig. S11*). RCTR1 was uncovered in self-limited infectious exudates as a mediator with novel capacities to protect host from collateral tissue damage, stimulate pro-resolving phagocyte functions, and enhance tissue regeneration (18). Its stereochemical structure and potent *in vivo* activities were established by matching physical properties and biological actions of synthetic RCTR1 to those of the endogenous material identified in mice and human tissues (18). The present results indicate that a GST as exemplified by LTC<sub>4</sub>S is involved in the biosynthesis of RCTR1 (*SI Appendix, Figs. S2 and S9*). Both LTC<sub>4</sub>S and GSTM3 are present in human neutrophils (*n* = 4) (36).

As leads and biotemplates for endogenous mediators in resolution of inflammation, resolvins and SPMs are gaining considerable interest and are opening new therapeutic avenues for the treatment and management of a wide range of inflammation-associated diseases including pulmonary diseases (37). To this end, resolvin D1 and D2 each demonstrate potent beneficial and regulatory actions on SARS-CoV-2-induced inflammation in cystic fibrosis macrophages (38). SPMs and resolvins alleviate chronic pain and itch via transient receptor potential regulation (11, 39), and it was documented that these autacoids preserve retinal structure and function in rats with retinitis (40). A recent human population study of 978 young adults associated adiposity with lower plasma resolvin E1 (41), suggesting the important roles of pro-resolving mediators in vascular and other chronic disorders. Temporal production of D-series resolvins in nanogram amounts by the salmon head kidney gland (42) illustrates the evolutionary significance of these conserved structures. Together, this body of literature highlights the critical role of elucidating stereochemical and biosynthetic mechanisms that produce SPMs and underscores the opportunity to harness the therapeutic potential of resolvins and their mimetics for novel approaches to treat disorders associated with excessive inflammation.

In summation, our present results galvanize the critical role of the resolvin 7,8(S,S)-epoxytetraene transient intermediate in the stereoselective biosynthesis of potent inflammation stop-signals, namely resolvin D1, resolvin D2, and RCTR1, by specific human leukocyte populations and recombinant enzymes. Together, these findings add essential components to our understanding of the omega-3 docosahexaenoate pathways that lead to the formation of potent bioactive molecules. They also underscore the significant role of allylic epoxide intermediates in the biosynthesis of autacoids by human leukocytes and offer insights integral to the potential development and exploration of resolution-based therapeutics.

## Methods

**Materials.** All recombinant enzymes, except leukotriene C<sub>4</sub> synthase (LTC<sub>4</sub>S) provided by J.Z.H., and synthetic lipid mediators used as standards for mass spectrometric analyses were purchased from Cayman Chemical Co. (Ann Arbor, MI). The sEH inhibitor N-[1-(1-oxopropyl)-4-piperidinyl]-N'-[4-(trifluoromethoxy)phenyl]-urea (TPPU), and LTC<sub>4</sub>S inhibitor 5-[[5-[(4-chlorophenyl)(cyclopropylmethyl)amino]-2-pyridinyl]carbonyl]-2-(4-methoxybenzoyl)-benzoic acid (TK05) were also purchased from Cayman Chemical. H<sub>2</sub><sup>18</sup>O was purchased from Cambridge Isotope Laboratories (CIL) (Tewksbury, MA).

**Stereoselective Total Synthesis of Resolvin 7,8(S,S)-Epoxytetraene.** The 7,8(S,S)-epoxytetraene used in our studies was obtained from two independent and convergent total organic syntheses. The first approach involved a triethylsilyl (TES)-protected-7,8(S,S)-epoxytetraene methyl ester synthetic intermediate. The purity of this material was >99% as judged by straight phase HPLC carried out using Agilent 1260 Infinity instrument (Agilent Technologies, Santa Clara, CA)

equipped with a binary pump and diode array detector (DAD) on a Luna 5 μm Silica(2) 100 Å, 250 × 10 mm (Phenomenex, Torrance, CA). A detailed account of the synthesis will be disclosed elsewhere. The second synthesis used a *tert*-butyldiphenylsilyl (TBDPS)-protected-7,8(S,S)-epoxytetraene methyl ester (22). Prior to incubations, both TES and TBDPS protective groups were each removed under <sup>t</sup>Bu<sub>4</sub>NF/AcOH conditions, followed by LiOH-based methyl ester hydrolysis. Both allylic epoxides matched their physical properties such as UV absorbance spectra and gave similar biosynthetic products from isolated leukocytes, recombinant enzymes, and nonenzymatic aqueous hydrolysis.

**Human PMN Isolation.** Human blood was collected with heparin (10 U/mL) from healthy volunteers, as approved by the Mass General Brigham IRB (protocol No. 1999P001297). PMNs were isolated by density gradient using Ficoll-histopaque (Sigma-Aldrich, 10771) as reported earlier (23), and all leukocyte preparations were deidentified before the experiments.

**Human PBMC Isolation.** Human PBMCs were obtained from deidentified leukopacks from Boston Children's Hospital Blood Bank (Boston, MA) under protocol No. 1999-P-001279 approved by the Mass General Brigham IRB prior to these experiments. PBMCs were isolated by Ficoll-Histopaque-1077 density-gradient.

**Human Macrophage Polarization and Differentiation.** Monocytes were purified from human PBMC fractions by adhesion. Monocytes were differentiated for 7 d in RPMI 1640 (Lonza) containing 10% fetal calf serum (ThermoFisher Scientific, 16000-044), 2 mM L-glutamine (Lonza, 17-605E), 2 mM penicillin-streptomycin (Lonza, 17-602E), and either 20 ng/mL of recombinant human macrophage colony-stimulating factor (hr-MCSF) (PeproTech, 300-25) for M2 macrophages or 20 ng/mL of GM-CSF (PeproTech, 300-03) for M1 macrophages at 37 °C. Macrophages were then polarized into M2 macrophages with 20 ng/mL of IL-4 (PeproTech, 200-04) or into M1 macrophages with 20 ng/mL of IFN-γ (PeproTech, 200-04) and 100 ng/mL of LPS for 48 h (23). For details, see (*SI Appendix, Fig. S5*).

**Flow Cytometry.** Human PBMC-derived M2-like macrophages were enumerated and assessed for viability by Trypan blue (Thermo Fisher) followed by fixation with a 4% paraformaldehyde solution (Electron Microscopy Sciences, Hatfield, PA). FcR-mediated, nonspecific antibody binding was blocked with Human TruStain FcX solution (422302; BioLegend). Human M2-like macrophages were stained with either M2 marker anti-human APC-conjugated CD206 (clone 19.2; 550889; BD Biosciences) and anti-human PE-conjugated CD163 (clone GHI/61; 333606; BioLegend) for 1 h. PBMCs were stained with anti-human APC/Cy7-conjugated CD3 (clone SK7; 557832; BD Biosciences), anti-human PE/Cy7-conjugated CD19 (clone HIB19; 302216; BioLegend), anti-human APC-conjugated CD16 (clone G2G8; 302012; BioLegend), anti-human FITC-conjugated CD14 (clone 6103; 11-0149-42; eBiosciences), anti-human Pacific blue-conjugated CD4 (clone OKT4; 317429; BioLegend), anti-human Alexa-fluor 700-conjugated CD8 (clone SK1, 344724, BioLegend) and anti-human PE-conjugated FoxP3 (clone 236A/E7, 12-4777-73, eBiosciences). Samples were acquired on a BD LSRFortessa (BD Biosciences) and analyzed with FlowJo software version X (FlowJo, Ashland, OR). Debris [forward scatter (FSC)-area (A) vs. side scatter (SSC)-A] and cellular doublets (FSC-height (H) vs. FSC-A → FSC-A vs. FSC-width (W) → SSC-H vs. SSC-A) were excluded before further gating on macrophage or PBMC markers. Unstained and secondary-only controls were used for differentiating macrophage vs. antibody fluorescence as well as single-stain controls for calculating compensation of fluorochrome wavelength overlap. For details, see (*SI Appendix, Figs. S5 and S6*).

**Incubations and Product Analysis.** All incubations with isolated human leukocytes and recombinant enzymes were performed at 37 °C for 30 min. The cytosolic (soluble) epoxide hydrolase (0.2 μM) was incubated with 5 μM of synthetic 7,8(S,S)-epoxytetraene in Tris-buffered saline (20 mM Tris, 100 mM KCl, pH 8). Studies with LTC<sub>4</sub>S were carried out in 25 mM Tris buffer containing reduced glutathione (10 equivalents) and 0.05% Triton X-100 at pH 8. Potato 5-LOX incubations were carried out in phosphate buffer (25 mM K<sub>2</sub>HPO<sub>4</sub>, 2 mM CaCl<sub>2</sub>, 1 mM ATP, pH = 7.4), whereas LTA<sub>4</sub>H studies were performed in a 10 mM Tris, 100 mM KCl buffer at pH 8. Prior to incubation experiments, UV spectra of substrates were recorded to assess compound integrity and obtain stoichiometric measurements. Reactions were stopped by two volumes of cold methanol followed by centrifugation (17,000 × g, 4 °C, 10 to 15 min), before mass spectrometric analyses. Products were analyzed and evaluated using relative percent ratios of multiple reaction monitoring (MRM) chromatograms.

**Incorporation of  $^{18}\text{O}$  from  $\text{H}_2^{18}\text{O}$ .** As discussed above, human recombinant sEH (0.2  $\mu\text{M}$ ) was incubated with the 7,8(S,S)-epoxytetraene (5  $\mu\text{M}$ ) at 37 °C for 30 min directly in  $^{18}\text{O}$ -enriched water (CIL) or in a 1:1 mixture with Tris-buffer (pH 8, 37 °C, 30 min).

**LC-MS/MS.** LC-MS/MS data were acquired on a triple quadrupole 7500 mass spectrometer (SCIEX, Framingham, MA). The instrument was equipped with an ExionLC system (SCIEX) and a Kinetex<sup>®</sup> 2.6  $\mu\text{m}$  PS C18 100 Å, 100 × 3.0 mm column (Phenomenex, Torrance, CA) maintained at 50 °C. The mobile phase composition consisted of solvent A ( $\text{H}_2\text{O}$ , 0.1% formic acid) and solvent B ( $\text{CH}_3\text{OH}$ , 0.1% formic acid). Using a 0.5 mL/min flow rate, the initial eluent mixture consisted of solvent A/solvent B (55/45, v/v) from 0 to 2 min. Then analytes were subjected to a gradient elution of 45 to 80% solvent B from 2 to 16.5 min. The next segment was increased from 80 to 98% between 16.5 and 16.6 min and was maintained at 98% of solvent B until 18.5 min. The final segment consisted of 10% solvent B from 18.6 to 20.9 min (*SI Appendix, Table S1*).

Source and gas parameters were programmed as follows: collision gas = 12, curtain gas = 40, ion source gas 1 (psi) = 45, ion source gas 2 (psi) = 70, ion spray voltage (V) = 2,000 (negative mode); 1,700 (positive mode), and source temperature (°C) = 500 (negative mode); 250 (positive mode). Resolvins D1 and D2 were monitored in negative ionization mode using  $m/z$  375 > 215 and  $m/z$  375 > 141 mass transitions, whereas RCT1 was detected in positive polarity using 666 > 548, 666 > 630, and 666 > 506 transitions. Data were obtained and analyzed using SCIEX OS 3.1.5.3945. These data are presented as screen captures. It should be noted that the accuracy for data resolution on SCIEX triple quad 7500 is 0.1 atomic mass units (a.m.u); the additional digits presented in mass spectra are the default manufacturer settings that cannot be changed. Ultra-violet (UV) absorbance spectra were recorded on the Agilent 1260 Infinity HPLC system, and on Cary 3500 Compact Peltier UV-vis Spectrophotometer (Agilent Technologies, Santa Clara, CA).

**MS<sup>3</sup> Studies.** MS/MS/MS ( $\text{MS}^3$ ) experiments were performed on the SCIEX Triple Quad 7500 system under the indicated LC conditions (*SI Appendix, Table S1*). An excitation energy (Auxiliary Frequency 2, AF2) of 0.1 (V) was utilized to investigate product diagnostic ions of interest.

**Molecular Docking Simulations.** Interaction sites between 5-LOX and DHA, 17-H(p)DHA or 17-HDHA were predicted via docking simulations using the 5-LOX crystal structure in a complex with arachidonic acid (AA) (PDB ID: 3V99) as a template. Interaction sites between human sEH and the 7,8(S,S)-epoxytetraene were predicted via docking simulations using sEH in a complex with 4-(3-cyclohexylurido)-heptanoic acid complex (PDB ID: 1ZD5) as a template. Ligands were prepared using the GradeWeb Server (<https://www.globalphasing.com>). Prior to docking, all ligands, except the catalytic iron, were removed from the crystal structures.

**Software.** Chemical structures were drawn using ChemDraw Level Professional v20.1.0.112 and Chem3D v21.0.0 (PerkinElmer, Waltham, MA). Computational simulations were visualized using the UCSF Chimera software v1.17.

**Statistical Analysis.** Significance was determined with the use of Student's *t* test. Analysis was conducted with GraphPad Prism version 9 (GraphPad Software, La Jolla, CA). Statistical significance was set at *P* values < 0.05.

**Data, Materials, and Software Availability.** Supporting LC-MS/MS raw data files are available in the BioStudies database (<https://www.ebi.ac.uk/biostudies/>) (43). All other data are included in the manuscript and/or *SI Appendix*.

**ACKNOWLEDGMENTS.** We thank Mary H. Small for expert assistance in preparation of the manuscript. We thank Dr. Ashley E. Shay for assessing LTC<sub>4</sub>S and GSTM1 to GSTM4 in human leukocytes. C.N.S. gratefully acknowledges support from the NIH (grant 5R35GM139430). J.Z.H. was supported by the Swedish Research Council (2023-02312).

Author affiliations: <sup>a</sup>Center for Experimental Therapeutics and Reperfusion Injury, Department of Anesthesiology, Perioperative and Pain Medicine, Brigham and Women's Hospital and Harvard Medical School, Boston, MA 02115; <sup>b</sup>Division of Physiological Chemistry II, Department of Medical Biochemistry and Biophysics, Karolinska Institute, Stockholm S-171 77, Sweden; and <sup>c</sup>Department of Cell Biology and Neuroscience, Virtua Health College of Medicine & Life Sciences of Rowan University, Stratford, NJ 08084

1. C. Nathan, Nonresolving inflammation redux. *Immunity* **55**, 592–605 (2022), 10.1016/j.immuni.2022.03.016.
2. C. N. Serhan *et al.*, Resolvins: A family of bioactive products of omega-3 fatty acid transformation circuits initiated by aspirin treatment that counter proinflammation signals. *J. Exp. Med.* **196**, 1025–1037 (2002), 10.1084/jem.20020760.
3. C. N. Serhan, Pro-resolving lipid mediators are leads for resolution physiology. *Nature* **510**, 92–101 (2014), 10.1038/nature13479.
4. G. Majno, I. Joris, *Cells, Tissues, and Disease: Principles of General Pathology* (Oxford University Press, New York, ed. 2, 2004).
5. A. Marfat, E. J. Corey, "Synthesis and structure elucidation of leukotrienes" in *Advances in Prostaglandin, Thromboxane, and Leukotriene Research*, J. E. Pike, D. R. Morton Jr., Eds. (Raven Press, New York, 1985), pp. 155–228.
6. B. Samuelsson, S. Hammarström, M. Hamberg, C. N. Serhan, "Structural determination of leukotrienes and lipoxins" in *Advances in Prostaglandin, Thromboxane, and Leukotriene Research*, J. E. Pike, D. R. Morton Jr., Eds. (Raven Press, New York, 1985), pp. 45–71.
7. B. Samuelsson, Role of basic science in the development of new medicines: Examples from the eicosanoid field. *J. Biol. Chem.* **287**, 10070–10080 (2012).
8. A. E. Shay *et al.*, Human leukocytes selectively convert 4S, 5S-epoxy-resolvin to resolvin D3, resolvin D4, and a Cys-resolvin isomer. *Proc. Natl. Acad. Sci. U.S.A.* **118**, e2116559118 (2021), 10.1073/pnas.2116559118.
9. R. Nshimiyimana, T. F. Lam, S. Aggarwal, C. N. Serhan, N. A. Petasis, First stereoselective total synthesis of 4(S),5(S)-oxido-17(S)-hydroxy-6(E),8(E),10(Z),13(Z),15(E),19(Z)-docosahexaenoic acid, the biosynthetic precursor of resolvins D3 and D4. *RSC Adv.* **12**, 11613–11618 (2022), 10.1039/d2ra01537d.
10. Y. P. Sun *et al.*, Resolvin D1 and its aspirin-triggered 17R epimer: Stereochemical assignments, anti-inflammatory properties, and enzymatic inactivation. *J. Biol. Chem.* **282**, 9323–9334 (2007), 10.1074/jbc.M609212200.
11. R. R. Ji, Specialized pro-resolving mediators as resolution pharmacology for the control of pain and itch. *Annu. Rev. Pharmacol. Toxicol.* **63**, 273–293 (2023), 10.1146/annurev-pharmtox-051921-084047.
12. C. López-Vicario *et al.*, Essential lipid autacoids rewire mitochondrial energy efficiency in metabolic dysfunction-associated fatty liver disease. *Hepatology* **77**, 1303–1318 (2023), 10.1002/hep.32647.
13. H. A. Bazan *et al.*, Circulating inflammation-resolving lipid mediators RvD1 and DHA are decreased in patients with acutely symptomatic carotid disease. *Prostaglandins Leukot. Essent. Fatty Acids* **125**, 43–47 (2017), 10.1016/j.plefa.2017.08.007.
14. D. Yu *et al.*, Declined serum resolvin D1 levels to predict severity and prognosis of human aneurysmal subarachnoid hemorrhage: A prospective cohort study. *Neuropsychiatr. Dis. Treat.* **19**, 1463–1476 (2023), 10.2147/ndt.s417630.
15. W. Li, H. Shan, Y. Ma, X. Lv, S. Zhu, Prognostic significance of serum resolvin D1 levels in patients with acute supratentorial intracerebral hemorrhage: A prospective longitudinal cohort study. *Clin. Chim. Acta* **547**, 117446 (2023), 10.1016/j.cca.2023.117446.
16. M. Spite, G. Fredman, Insights into the role of the resolvin D2-GPR18 signaling axis in cardiovascular physiology and disease. *Adv. Pharmacol.* **97**, 257–281 (2023), 10.1016/bs.apha.2022.12.005.
17. B. Liu *et al.*, Inverted U-shaped association of plasma resolvin D2 with atherosclerotic cardiovascular disease and the mediation effects of serum cholesterol: A Chinese community-based study. *J. Am. Heart Assoc.* **13**, e032588 (2024), 10.1161/JAHA.123.032588.
18. X. de la Rosa *et al.*, Identification and complete stereochemical assignments of the new resolvin conjugates in tissue regeneration in human tissues that stimulate proresolving phagocyte functions and tissue regeneration. *Am. J. Pathol.* **188**, 950–966 (2018), 10.1016/j.ajpath.2018.01.004.
19. S. Deyama *et al.*, Resolvin D1 and D2 reverse lipopolysaccharide-induced depression-like behaviors through the MTORC1 signaling pathway. *Int. J. Neuropsychopharmacol.* **20**, 575–584 (2017), 10.1093/ijnp/pyx023.
20. J. J. Velasco, F. G. Akar, A new year's resolution to resolve atrial fibrillation: Resolvin D1 emerges as a powerful target against post-MI atrial remodeling. *Cardiovasc. Res.*, 10.1093/cvr/cvae039 (2024).
21. Q. Yang *et al.*, Resolvin conjugates in tissue regeneration 1 promote alveolar fluid clearance by activating alveolar epithelial sodium channels and Na, K-ATPase in lipopolysaccharide-induced acute lung injury. *J. Pharmacol. Exp. Ther.* **379**, 156–165 (2021), 10.1124/jpet.121.000712.
22. A. R. Rodriguez, B. W. Spur, First total synthesis of pro-resolving and tissue-regenerative resolvin sulfido-conjugates. *Tetrahedron Lett.* **58**, 1662–1668 (2017), 10.1016/j.tetlet.2017.03.041.
23. R. Nshimiyimana *et al.*, Stereochemistry and functions of the new cysteinyl-resolvin, 4S,5R-RCT1, in efferocytosis and erythrophagocytosis of human senescent erythrocytes. *Am. J. Hematol.* **98**, 1000–1016 (2023), 10.1002/ajh.26932.
24. J. Z. Haegström, M. E. Newcomer, Structures of leukotriene biosynthetic enzymes and development of new therapeutics. *Annu. Rev. Pharmacol. Toxicol.* **63**, 407–428 (2023), 10.1146/annurev-pharmtox-051921-085014.
25. S. Hong *et al.*, Novel docosatrienes and 17S-resolvins generated from docosahexaenoic acid in murine brain, human blood, and glial cells: Autacoids in anti-inflammation. *J. Biol. Chem.* **278**, 14677–14687 (2003), 10.1074/jbc.M300218200.
26. R. W. Egan *et al.*, "Specific inhibition and oxidative regulation of 5-lipoxygenase" in *Advances in Prostaglandin, Thromboxane, and Leukotriene Research*, B. Samuelsson, R. Paoletti, P. W. Ramwell, Eds. (Raven Press, New York, 1983), pp. 151–157.
27. J. Haegström *et al.*, Enzymatic formation of 5,6-dihydroxy-7,9,11,14-eicosatetraenoic acid: Kinetics of the reaction and stereochemistry of the product. *Biochim. Biophys. Acta* **958**, 469–476 (1988), 10.1016/0005-2760(88)90233-0.
28. M. Spite *et al.*, Resolvin D2 is a potent regulator of leukocytes and controls microbial sepsis. *Nature* **461**, 1287–1291 (2009), 10.1038/nature08541.
29. T. Shimizu *et al.*, Enzyme with dual lipoxygenase activities catalyzes leukotriene A4 synthesis from arachidonic acid. *Proc. Natl. Acad. Sci. U.S.A.* **81**, 689–693 (1984), 10.1073/pnas.81.3.689.
30. E. J. Corey, M. M. Mehrotra, A stereoselective and practical synthesis of 5,6(S,S)-epoxy-15(S)-hydroxy-7(E),9(E),11(Z),13(E)-eicosatetraenoic acid (4), possible precursor of the lipoxins. *Tetrahedron Lett.* **27**, 5173–5176 (1986), 10.1016/S0040-4039(00)85161-8.

31. J. Seidegard *et al.*, Measurement and characterization of membrane-bound and soluble epoxide hydrolase activities in resting mononuclear leukocytes from human blood. *Cancer Res.* **44**, 3654–3660 (1984).
32. H. B. Abdalla *et al.*, Soluble epoxide hydrolase inhibition enhances production of specialized pro-resolving lipid mediator and promotes macrophage plasticity. *Br. J. Pharmacol.* **180**, 1597–1615 (2023), 10.1111/bph.16009.
33. V. Schmitz Nunes *et al.*, Insights into the activation mechanism of the ALX/FPR2 receptor. *J. Phys. Chem. Lett.* **11**, 8952–8957 (2020), 10.1021/acs.jpclett.0c02052.
34. H. Arnardottir *et al.*, The resolvin D1 receptor GPR32 transduces inflammation resolution and atheroprotection. *J. Clin. Invest.* **131**, e142883 (2021), 10.1172/JCI142883.
35. N. Chiang *et al.*, Identification of resolvin D2 receptor mediating resolution of infections and organ protection. *J. Exp. Med.* **212**, 1203–1217 (2015), 10.1084/jem.20150225.
36. C. C. Jouvene *et al.*, Biosynthetic metabolomes of cysteinyl-containing immunoresolvents. *FASEB J.* **33**, 13794–13807 (2019), 10.1096/fj.201902003R.
37. D. Centanni, P. A. J. Henricks, F. Engels, The therapeutic potential of resolvins in pulmonary diseases. *Eur. J. Pharmacol.* **958**, 176047 (2023), 10.1016/j.ejphar.2023.176047.
38. A. Recchiuti *et al.*, Resolvin D1 and D2 reduce SARS-CoV-2-induced inflammatory responses in cystic fibrosis macrophages. *FASEB J.* **35**, e21441 (2021), 10.1096/fj.202001952R.
39. J. Roh *et al.*, Resolvins: Potent pain inhibiting lipid mediators via transient receptor potential regulation. *Front. Cell Dev. Biol.* **8**, 1–15 (2020), 10.3389/fcell.2020.584206.
40. A. J. Mead *et al.*, Loss of 15-lipoxygenase in retinodegenerative RCS rats. *Int. J. Mol. Sci.* **25**, 1–19 (2024), 10.3390/ijms25042309.
41. A. Barden *et al.*, Adiposity associates with lower plasma resolvin E1 (Rve1): A population study. *Int. J. Obes. (Lond.)*, 10.1038/s41366-024-01482-x (2024).
42. P. Araujo, S. Iqbal, A. Arnø, M. Espe, E. Holen, Validation of a liquid–liquid extraction method to study the temporal production of D-series resolvins by head kidney cells from Atlantic salmon (*Salmon salar*) exposed to docosahexaenoic acid. *Molecules* **28**, 4728 (2023), 10.3390/molecules28124728.
43. R. Nshimiyimana, C. N. Serhan, Raw dataset from “Biosynthesis of resolvin D1, resolvin D2, and RCTR1 from 7,8(S,S)-epoxytetraene in human neutrophils and macrophages”. BioStudies. <https://www.ebi.ac.uk/biostudies/studies/S-BSST1612>. Deposited 21 August 2024.